Hindawi
Shock and Vibration
Volume 2018, Article ID 6476783, 16 pages
https://doi.org/10.1155/2018/6476783

Research Article

Damping Identification with Acceleration Measurements Based on Sensitivity Enhancement Method

Xusheng Wang,[1] Kun Liu ,[2] Hongbo Liu,[3] and Yuhan He[4]

[1]*Key Lab of Structures Dynamics Behavior and Control of the Ministry of Education, Harbin Institute of Technology, Harbin 150090, China*
[2]*Key Lab of Smart Prevention and Mitigation of Civil Engineering Disasters of the Ministry of Industry and Information Technology, Harbin Institute of Technology, Harbin 150090, China*
[3]*School of Civil Engineering and Architecture, Heilongjiang University, Harbin 150080, China*
[4]*School of Civil Engineering and Architecture, University of Jinan, Jinan 250022, China*

Correspondence should be addressed to Kun Liu; kun.liu@hit.edu.cn

Received 12 February 2018; Accepted 15 May 2018; Published 12 June 2018

Academic Editor: Emanuele Reccia

The damping is important for forward and inverse structural dynamic analysis, and damping identification has become a hot issue in structural health monitoring recently. The dynamic responses of the structure can be measured in practice, and the structural parameter usually can be identified by inverse response sensitivity analysis. To reduce the measurement noise effect and enhance the effectiveness of the response sensitivity method, an enhanced sensitivity analysis method was proposed to identify the structural damping based on the Principal Component Analysis (PCA) method. The measured acceleration responses were analyzed by PCA method, and the updated analytical responses and the response sensitivities were projected into the subspace determined by the first-order principal component. The projection equations were adopted to identify the parameters of damping model. The proposed damping identification method was numerically validated with a planar truss structure at first, and then the experimental study was conducted with a steel planar frame structure. It shows that the proposed method is effective in identifying the parameters of damping model with better accuracy compared with the conventional acceleration response sensitivity method, and it is also robust to the sensor placement and measurement noise.

1. Introduction

The damping ratio is a dimensionless measure and a measure of describing how rapidly the oscillations of a structural system decay from one bounce to the next, which is a significant factor when analyzing the structural dynamic behavior dominated by energy dissipation [1]. Unlike the mass or stiffness that can be measured or determined by static test, the damping cannot be determined by measurement or static test [2], but the damping characteristic is very important in structural health monitoring. Accurate damping matrix construction is a determining factor in analyzing structural dynamic responses and predicting energy dissipation behavior, which makes the damping estimation become a key issue for the structural design, dynamic response analysis, structural health monitoring, etc.

In order to construct accurate structural damping matrix, damping identification has been studied by some researchers for different systems, including rotor systems [3], mistuned blisks [4] and monopile foundation [5]. For the structural system, the damping identification method can be classified into frequency domain method [6–8], time domain method [9–11], and time-frequency domain method [12, 13]. The half-power bandwidth method [6, 7] in frequency domain is usually adopted in the dynamic test, and Wang [8] studied the errors of calculating damping effect between the classical and the third-order half-power method. Li and Law [9] proposed a time domain damping ratio identification method based on the acceleration response sensitivity, and the proposed method is validated by numerical study and experimental study [11]. The time domain response sensitivity method was combined with iterative regularization method to identify

damping ratios [10]. The wavelet analysis method [12, 13] and Hilbert–Huang Transform method [14] have also been adopted to identify the damping ratio.

Sensitivity analysis can be used to estimate the system output variation due to a perturbation in the system parameters by means of partial derivatives [15, 16], and forward sensitivity analysis has been used in many applications [17–19]. Inverse sensitivity-based method with model updating is usually based on a first-order Taylor series that minimizes an error function to assess the system parameter perturbation, and time domain sensitivity method has been adopted in structural parameter identification widely [20–22]. The time domain response sensitivity method has advantages including no requirement of computing the higher order system model parameters, obtaining the responses easily, and providing more identification equations, which makes it a good tool for damping identification. Time domain response sensitivity method has also been studied and gained significant attention in damping identification [9–11].

The time domain response sensitivity method also has the disadvantage of being sensitive to the measurement noise [23, 24], and it is also important to enhance the response sensitivity for the structural parameter identification [24–26]. The Principal Component Analysis (PCA) technique, also known as Karhunen-Loeve transform or proper orthogonal decomposition [27], decomposes data series through orthogonal linear transformation to get the principal components, the first few of which contain more information of the parameter variation and less random noise information. The relationship between the system parameters and its output has been broadly studied with a combination of sensitivity analysis and Principal Component Analysis (PCA) [28, 29], and it has been proved that PCA method can improve the response sensitivity for structural damage identification [25, 26] with subspace projection method.

With the rapid development of measurement technique, the time domain responses of the structure can be obtained, and the acceleration responses of the structure can be measured easily. This paper will propose a damping identification method based on the acceleration response measurement. The inverse acceleration response sensitivity method for damping ratio identification is revisited, and the model updating method is also briefly reviewed in this paper at first. The measured acceleration responses are decomposed by PCA method, and time domain response sensitivity equations of damping ratio identification are projected into the finer subspace. With the iterative procedure of model updating and subspace projection, the enhanced sensitivity method is proposed to identify the parameters of damping model. The proposed method is described in detail, and it is validated with simulation studies on a plane truss structure, in which different sensor placements and different measurement noise levels are studied. A seven-storey steel frame was designed and manufactured in the laboratory, and hammer test was performed. The proposed acceleration response sensitivity enhancement method is used to identify the damping ratio of the steel frame structure.

2. Methodology

2.1. Damping Identification Based on Acceleration Response Sensitivity. The equation of motion of a damped linear structure can be written as

$$\mathbf{M}\ddot{\mathbf{x}} + \mathbf{C}\dot{\mathbf{x}} + \mathbf{K}\mathbf{x} = \mathbf{L}\mathbf{P}(t) \tag{1}$$

where $\mathbf{M}$, $\mathbf{C}$, and $\mathbf{K}$ are the mass, damping, and stiffness matrices of the structural system, respectively. $\mathbf{P}(t)$ is the vector of excitations on the structure and $\mathbf{L}$ is the mapping matrix for the excitations. $\ddot{\mathbf{x}}$, $\dot{\mathbf{x}}$, and $\mathbf{x}$ are vectors of the acceleration, velocity, and displacement responses, respectively.

Performing differentiation to both sides of (1) with respect to damping ratio ζ_j, which is the critical parameter in structural damping model, we have

$$\mathbf{M}\frac{\partial \ddot{\mathbf{x}}}{\partial \zeta_j} + \mathbf{C}\frac{\partial \dot{\mathbf{x}}}{\partial \zeta_j} + \mathbf{K}\frac{\partial \mathbf{x}}{\partial \zeta_j} = -\frac{\partial \mathbf{C}}{\partial \zeta_j}\dot{\mathbf{x}} \tag{2}$$

where ζ_j is the jth damping ratio of the structural system, and $\partial\ddot{\mathbf{x}}/\partial\zeta_j$, $\partial\dot{\mathbf{x}}/\partial\zeta_j$, and $\partial\mathbf{x}/\partial\zeta_j$ are the acceleration, velocity, and displacement sensitivity vectors, respectively, which can be determined by *Newmark-β* method solving (2).

The acceleration sensitivity vector corresponding to jth damping ratio can be rewritten as $\mathbf{S}_{\zeta_j}$. All the sensitivity vectors are assembled as

$$\mathbf{S} = \left[\mathbf{S}_{\zeta_1} \ \cdots \ \mathbf{S}_{\zeta_j} \ \cdots \ \mathbf{S}_{\zeta_n}\right] \tag{3}$$

The identification equation for all the damping ratios of a structure can be represented as

$$\mathbf{S}\Delta\boldsymbol{\zeta} + o\left(\Delta\boldsymbol{\zeta}\right)^2 = \ddot{\mathbf{x}}_c - \ddot{\mathbf{x}}_m \tag{4}$$

The higher order term $o(\Delta\boldsymbol{\zeta})^2$ can be omitted in (4). With an iterative method the damping ratio perturbations can be determined from (4), and Tikhonov regularization is used for optimizing the following objective function in the kth iteration as

$$\mathrm{J}\left(\Delta\boldsymbol{\zeta}^k, \lambda_\zeta^k\right) = \left\|\mathbf{S}\Delta\zeta^k - \left(\ddot{\mathbf{x}}_c - \ddot{\mathbf{x}}_m\right)\right\|^2 + \lambda_\zeta^k \left\|\Delta\zeta^k\right\| \tag{5}$$

where λ_ζ^k is the regularization parameter in the kth iteration obtained with the L-curve method [30].

After $\Delta\zeta^k$ is solved, the damping matrix is updated with

$$\boldsymbol{\zeta}^k = \boldsymbol{\zeta}^0 + \sum_{i=1}^{k}\Delta\zeta^i \tag{6}$$

where $\boldsymbol{\zeta}^0$ is the assumed initial damping ratio vector.

Then after recalculating the structural responses and the sensitivity matrix, the vector $\boldsymbol{\zeta}^{k+1}$ for the next identification iteration is obtained until the given convergence criterion is met:

$$\frac{\left\|\boldsymbol{\zeta}^{k+1} - \boldsymbol{\zeta}^k\right\|}{\left\|\boldsymbol{\zeta}^{k+1}\right\|} < Tol \tag{7}$$

Tol values are selected to meet the challenge in convergence of the identified results with measurement noise effect, and then the final value of the damping ratio can be obtained.

2.2. Acceleration Response Sensitivity Enhancement by PCA. The initial structural damping ratio vector is assumed as $\boldsymbol{\zeta}^0$, and the initial analytical acceleration responses corresponding to $\boldsymbol{\zeta}^0$ in the initial stage can be determined from (1) with the *Newmark-β* method. The measured acceleration responses can be obtained with the accelerometers in the structure. Based on the initial analytical acceleration response vectors $\ddot{\mathbf{x}}_c^0$ and measured acceleration response vectors $\ddot{\mathbf{x}}_m$, the identification equation for the first identification iteration can be written as

$$\mathbf{S}\left(\boldsymbol{\zeta}^0\right)\Delta\boldsymbol{\zeta}^1 = \ddot{\mathbf{x}}_c^0 - \ddot{\mathbf{x}}_m \tag{8}$$

The PCA is applied to the measured acceleration responses $\ddot{\mathbf{x}}_m$, and the covariance matrix of $\ddot{\mathbf{x}}_m$ is $\mathrm{cov}(\ddot{\mathbf{x}}_m) = E((\ddot{\mathbf{x}}_m)(\ddot{\mathbf{x}}_m)^T)$, when written in the form of spectral decomposition as

$$\mathrm{cov}\left(\ddot{\mathbf{x}}_m\right) = \sum_{i=1}^{p} \lambda_i^m \mathbf{U}_i^m \left(\mathbf{U}_i^m\right)^T \tag{9}$$

where λ_i^m $(i = 1, \cdots, p)$ is the vector of eigenvalues of the covariance matrix; $\mathbf{U}_i^m$ $(i = 1, \cdots, p)$ is the corresponding eigenvector matrix which defines an orthogonal subspace; p is the number of measured acceleration responses here.

The principal components $\ddot{\mathbf{x}}_{m,i}$ $(i = 1, \cdots, p)$ of measured acceleration responses are then obtained as

$$\ddot{\mathbf{x}}_{m,i} = \left(\mathbf{U}_i^m\right)^T \ddot{\mathbf{x}}_m \quad \left(i = 1, \cdots, p\right) \tag{10}$$

The initial analytical responses can be projected into the subspace constructed by the eigenvector matrix $\mathbf{U}_i^m$ $(i = 1, \cdots, p)$ as

$$\ddot{\mathbf{x}}_{c,i} = \left(\mathbf{U}_i^m\right)^T \ddot{\mathbf{x}}_c^0 \quad \left(i = 1, \cdots, p\right) \tag{11}$$

The same projection can be conducted to the sensitivity vectors, so the projection of (8) with the same subspace can be written as

$$\left(\mathbf{U}_i^m\right)^T \mathbf{S}\left(\boldsymbol{\zeta}^0\right)\Delta\boldsymbol{\zeta}^1 = \left(\mathbf{U}_i^m\right)^T \ddot{\mathbf{x}}_c^0 - \ddot{\mathbf{x}}_m \quad \left(i = 1, \cdots, p\right) \tag{12}$$

The orthogonal vectors $\mathbf{U}_i^m$ insure each equation in (12) is independent in the subspace. The dimension of the projection sensitivity matrix for each principle component is $n_t \times n$, where n_t is the length of the measured acceleration and n is the number of the damping ratios. If there are r principal components selected for determining the damping ratios, the projection sensitivity matrix dimension becomes $(r \times n_t) \times n$.

The principal components, which contain less measured noise information and most of the structural damping perturbation information, will be selected, and the selection of principal components will be discussed in next section. Then the damping ratio perturbation $\Delta\boldsymbol{\zeta}^1$ can be obtained by Tikhonov regularization method as (5) with the projection sensitivity equation in (12).

Similar to the conventional response sensitivity method [9], the model updating procedure is conducted when each damping ratio perturbation $\Delta\boldsymbol{\zeta}^j$ is determined in the jth iterative step. After each iteration step, the damping ratio is updated with (6), and the analytical acceleration and sensitivity matrix are updated. The procedure of the proposed method for damping ratios identification is presented as the following 5 steps.

Step 1. The measured acceleration responses are analyzed with the PCA method, and the principal components, which contain less measured noise information and more damping ratio perturbation information, are selected.

Step 2. Based on the finite element model and initial damping ratio, the corresponding analytical acceleration responses and sensitivity matrix are calculated with the *Newmark-β* method, and then the identification equation in (12) is determined based on (1)-(12).

Step 3. The identification equation is solved with Tikhonov regularization method to obtain the damping ratio perturbations.

Step 4. The damping ratio vector is updated, and with the new damping ratios, the damping matrix of the structural model is updated and the analytical responses and corresponding response sensitivity matrix are recalculated. The identification equation in (12) is determined based on (1)-(12) with the updated damping ratios.

Step 5. Step 3 to Step 4 are repeated, and the iterative process will stop until the convergence criterion defined in (6) is satisfied.

The flowchart of the proposed damping identification method is shown in Figure 1.

3. Numerical Simulation Study

3.1. Numerical Simulation Case. A two-dimensional truss structure as shown in Figure 2 serves for the numerical study. This structure is modeled using 61 truss finite elements, and each node consists of 2 *Dof*s including the translational displacements in horizontal and vertical directions. This structure is pin-supported at Node 1 and roller-supported at Node 25, and the node number and element number are also shown in Figure 2. Each vertical and horizontal member is of 1.0-meter length, and the cross-sectional area of all members is 0.0016 m^2. The Rayleigh damping model is adopted, which has two damping ratios needed to be identified.

The mass density of material and the elastic modulus of material are 7.8×10^3 $\mathrm{kg/m}^3$ and 2.06 GPa, respectively. The system mass and stiffness matrices can be established based on the geometry and material properties of the model. The first eight natural frequencies of the structure are 1.5792 Hz, 5.2627 Hz, 7.0661 Hz, 12.6623 Hz, 18.4986 Hz, 21.2952 Hz, 29.0158 Hz, and 32.3490 Hz, respectively.

It assumes that the real damping ratio coefficients associated with the first and second modes are 1% and 2% in the Rayleigh damping model, respectively. The truss structure is subjected to vertical and horizontal external dynamic forces

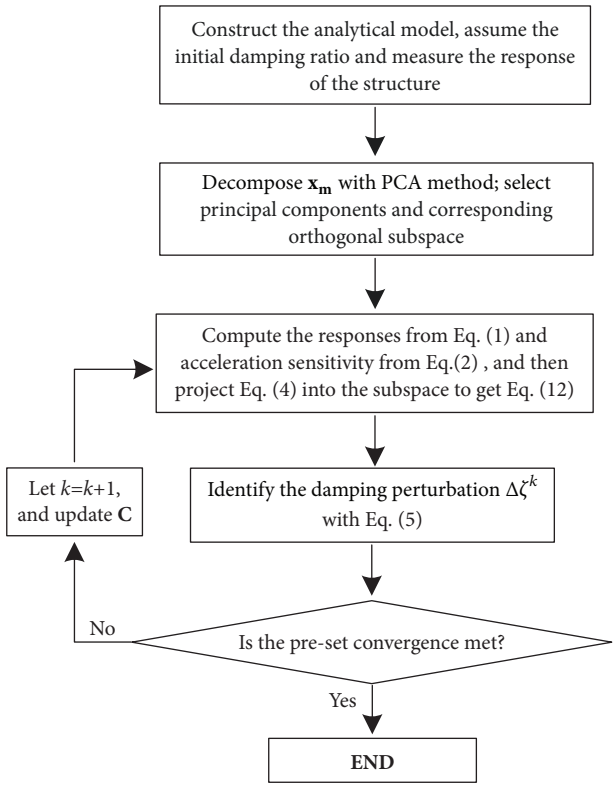

Figure 1: The flowchart of the proposed damping identification method.

as shown in (13), and the dynamic forces are modeled as follows to simulate excitations over a relatively wide range of frequencies.

$$\begin{aligned}\mathbf{F}_1 &= 65\sin(20\pi t) + 60\sin(30\pi t) + 55\sin(80\pi t)\\ \mathbf{F}_2 &= 60\sin(30\pi t) + 60\sin(70\pi t) + 50\sin(80\pi t)\end{aligned} \tag{13}$$

The accelerometers are set to collect acceleration responses of the structure, and the duration of measurement is 1.0 second with 1000 Hz sampling rate. The "measured responses" are simulated by adding random components to the "measured responses without noise effect" as

$$\ddot{\mathbf{x}}_m = \ddot{\mathbf{x}}_{mr} + \mathrm{E_p}\sigma\left(\ddot{\mathbf{x}}_{mr}\right)\mathbf{N}_{noise} \tag{14}$$

where $\ddot{\mathbf{x}}_{mr}$ is the "measured response without noise effect" which can be determined by *Newmark-β* method with the real damping ratio in numerical simulation; $\mathrm{E_p}$ is the noise level; $\sigma(\ddot{\mathbf{x}}_{mr})$ is the standard deviation of the "measured response without noise effect"; and $\mathbf{N}_{noise}$ is a vector of random values with zero mean and unit standard deviation.

It is impractical to measure the responses of all the *Dof*s in a real structure, and the measurement location will affect the identification result. This work will not discuss the sensor placement effect, and six arbitrarily selected sets of the sensors, which are shown in Table 1, are adopted to validate that the proposed damping identification method is robust to sensor placement.

Table 1: Sensor placements.

No. of Sensor Sets	Sensor Location
Sensor set 1	3x, 11x, 21x
Sensor set 2	3y, 11y, 21y
Sensor set 3	5x, 13x, 21x
Sensor set 4	5y, 13y, 21y
Sensor set 5	5x, 15x, 23x
Sensor set 6	5y, 15y, 23y

3.2. Damping Identification without Measurement Noise. Both of the initial damping ratio coefficients are assumed to be 3%. The structural responses are simulated with the *Newmark-β* method from the structure with the real damping ratios and initial damping ratios, in which the responses with the real damping ratios are considered as "measured responses without noise effect" and the responses with the initial damping ratios are considered as "initial analytical responses". The measurement noise is not considered in this case, so the "measured responses without noise effect" are adopted to identify the damping ratio in this section to validate the correctness of the proposed method.

The "measured responses without noise effect" from different sensor placement are decomposed by PCA method, and the corresponding "analytical responses" are projected into the subspace constructed by the principal components as (11). The damping ratios are identified with single principal component based on the "measured responses without noise effect", and the identified results from the proposed method with different sensor placements are listed in Table 2. It shows that the identified results match the real value perfectly indicating the correctness and good accuracy of the proposed method in damping identification, and it can be concluded that without considering the measurement noise the satisfactory identification results can be achieved based on every single component.

The PCA decompose time domain data series into principal components via orthogonal linear transformation, and the components corresponding to larger eigenvalues usually contain more information of the original data series. In order to study the perturbation information of damping ratio in the principal components of the measured responses, a ratio Δ_j is defined in (15) to present the relative perturbation information of damping ratio in different principal components.

$$\Delta_j = \frac{\left\|\mathbf{C}_{j,mr} - \mathbf{C}_{j,c}\right\|}{\left\|\ddot{\mathbf{x}}_{mr} - \ddot{\mathbf{x}}_c^0\right\|} \tag{15}$$

where $\|\mathbf{C}_{j,mr} - \mathbf{C}_{j,c}\|$ is the norm of the difference between the jth principal component of the "measured responses without noise effect" and the corresponding projected component of "initial analytical responses", and $\|\ddot{\mathbf{x}}_{mr} - \ddot{\mathbf{x}}_c^0\|$ is the norm of the difference between the "measured responses without noise effect" and "initial analytical responses".

All the ratios with different sensor placements are shown in Table 3. The ratios of the lower order principal component are usually larger than that of higher order principal components. It indicates that the lower order principal component

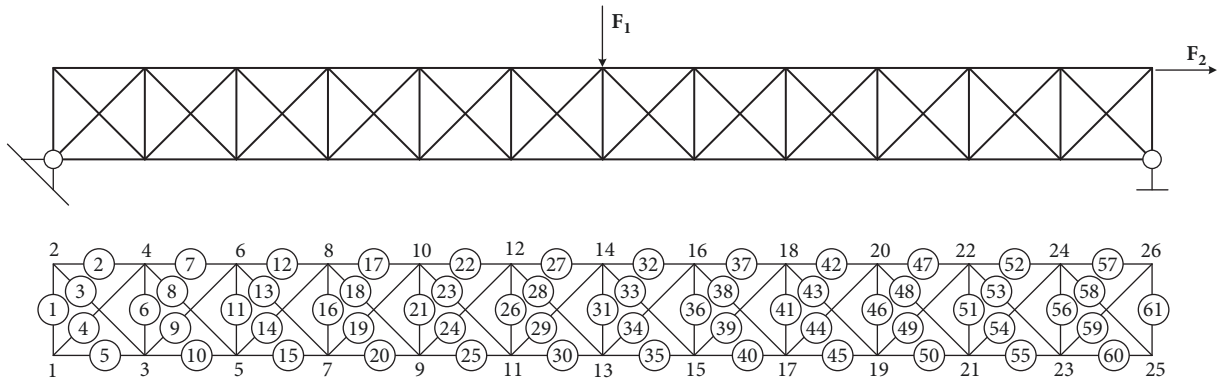

Figure 2: The plane truss structure.

Table 2: Identification results from single principal component without measurement noise effect.

Damping ratio	Sensor set 1			Sensor set 2			Sensor set 3		
	1st	2nd	3rd	1st	2nd	3rd	1st	2nd	3rd
ζ_1	0.01	0.01	0.01	0.01	0.01	0.01	0.01	0.01	0.01
ζ_2	0.02	0.02	0.02	0.02	0.02	0.02	0.02	0.02	0.02
Damping ratio	Sensor set 4			Sensor set 5			Sensor set 6		
	1st	2nd	3rd	1st	2nd	3rd	1st	2nd	3rd
ζ_1	0.01	0.01	0.01	0.01	0.01	0.01	0.01	0.01	0.01
ζ_2	0.02	0.02	0.02	0.02	0.02	0.02	0.02	0.02	0.02

Table 3: The ratio Δ for different principal components without measurement noise.

Δ	Sensor set 1	Sensor set 2	Sensor set 3	Sensor set 4	Sensor set 5	Sensor set 6
Δ_1	0.9774	0.7769	0.9194	0.9991	0.9763	0.7964
Δ_2	0.4764	0.8528	0.3361	0.4781	0.6614	0.8612
Δ_3	0.2699	0.5147	0.4898	0.1295	0.7052	0.4523

contains more perturbation information of damping ratios, which makes the lower order principal component better for damping ratio identification than higher order components.

3.3. Principal Components Selection for Damping Identification with Measurement Noise. In practice the measurement noise cannot be avoided, so the measurement noise effect should be considered in damping identification. All the principal components of the "measured responses without noise effect" can be used to identify the damping ratio with perfect accuracy, but the principal component will be affected by the measurement noise. In this section, the measurement noise information distribution in the principal component will be discussed, and the principal component selection criterion will be given.

Both of the initial damping ratio coefficients are also assumed to be 3% in this section. The structural responses are simulated with the *Newmark-β* method from the structure with the real damping ratios and initial damping ratios, in which random noise is added to the responses with the real damping ratios being considered as "measured responses". In this section 10% measurement noise is considered in damping ratio identification and the measurement noise information distribution in different principal components is discussed.

The "measured responses" from different sensor placement are decomposed by PCA method, and the corresponding "measured responses without noise effect" are projected into the subspace constructed by the principal components as (11). In order to study the measurement noise information in the principal components of the measured responses, a ratio δ_j is defined in (16) to present the measurement noise information distribution in different principal components.

$$\delta_j = \frac{\left\| \mathbf{C}_{j,m} - \mathbf{C}_{j,mr} \right\|}{\left\| \mathbf{C}_{j,mr} \right\|} \tag{16}$$

where $\|\mathbf{C}_{j,m} - \mathbf{C}_{j,mr}\|$ is the norm of the difference between the jth principal component of the "measured responses" and the corresponding projected component of "measured responses without noise effect".

Ten different measurement noise series are added to the "measured responses without noise effect" to simulate the "measured responses" as in (14), and the ratio defined in (16) is calculated. The values of δ_j with different measurement noise series are shown in Figure 3; it seems that the noise

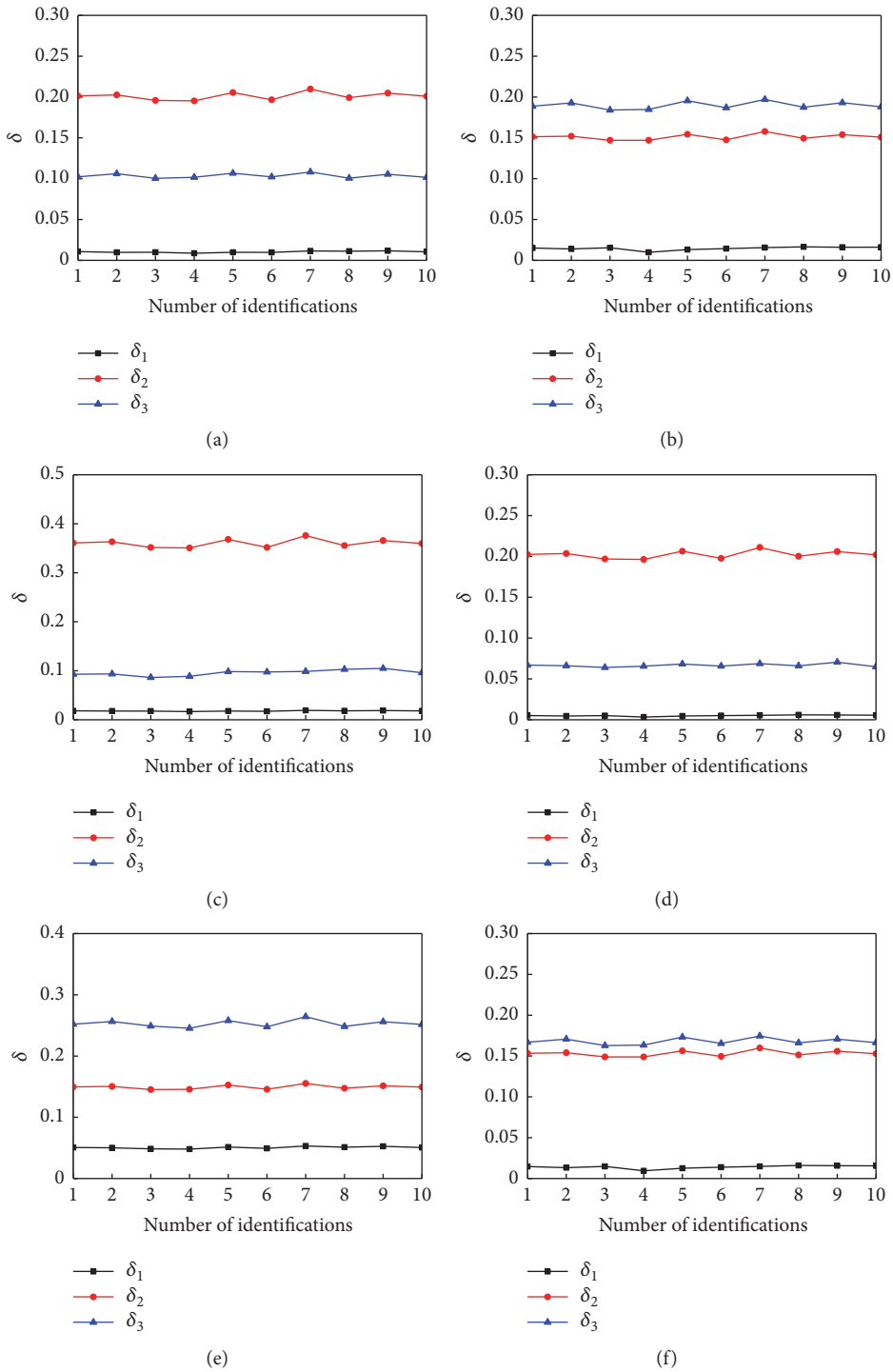

Figure 3: δ value with different sensor placement. (a) Sensor set 1. (b) Sensor set 2. (c) Sensor set 3. (d) Sensor set 4. (e) Sensor set 5. (f) Sensor set 6.

information distribution in every principal component is stable for all the sensor placements, in which the first principal component always contains least noise information. The mean values $\overline{\delta}_j$ for different sensor placements are shown in Table 4, and it can be seen that the lower order principal components are noted to be less affected by measurement noise.

In the last section, it has been proved that the lower order principal components of the "measured responses without noise effect" also usually contain more perturbation information of damping ratios. The "measured responses without noise effect" in (15) are replaced by "measured responses", and the values of Δ_j with different measurement noise series are shown in Figure 4. It can be seen that the perturbation

Table 4: The mean values of δ with 10% measurement noise.

$\overline{\delta}$	Sensor set 1	Sensor set 2	Sensor set 1	Sensor set 4	Sensor set 5	Sensor set 6
$\overline{\delta}_1$	1.03%	1.46%	1.79%	0.51%	5.05%	1.41%
$\overline{\delta}_2$	20.12%	15.11%	36.04%	20.22%	14.92%	15.31%
$\overline{\delta}_3$	10.35%	18.98%	9.6%	6.67%	25.28%	16.80%

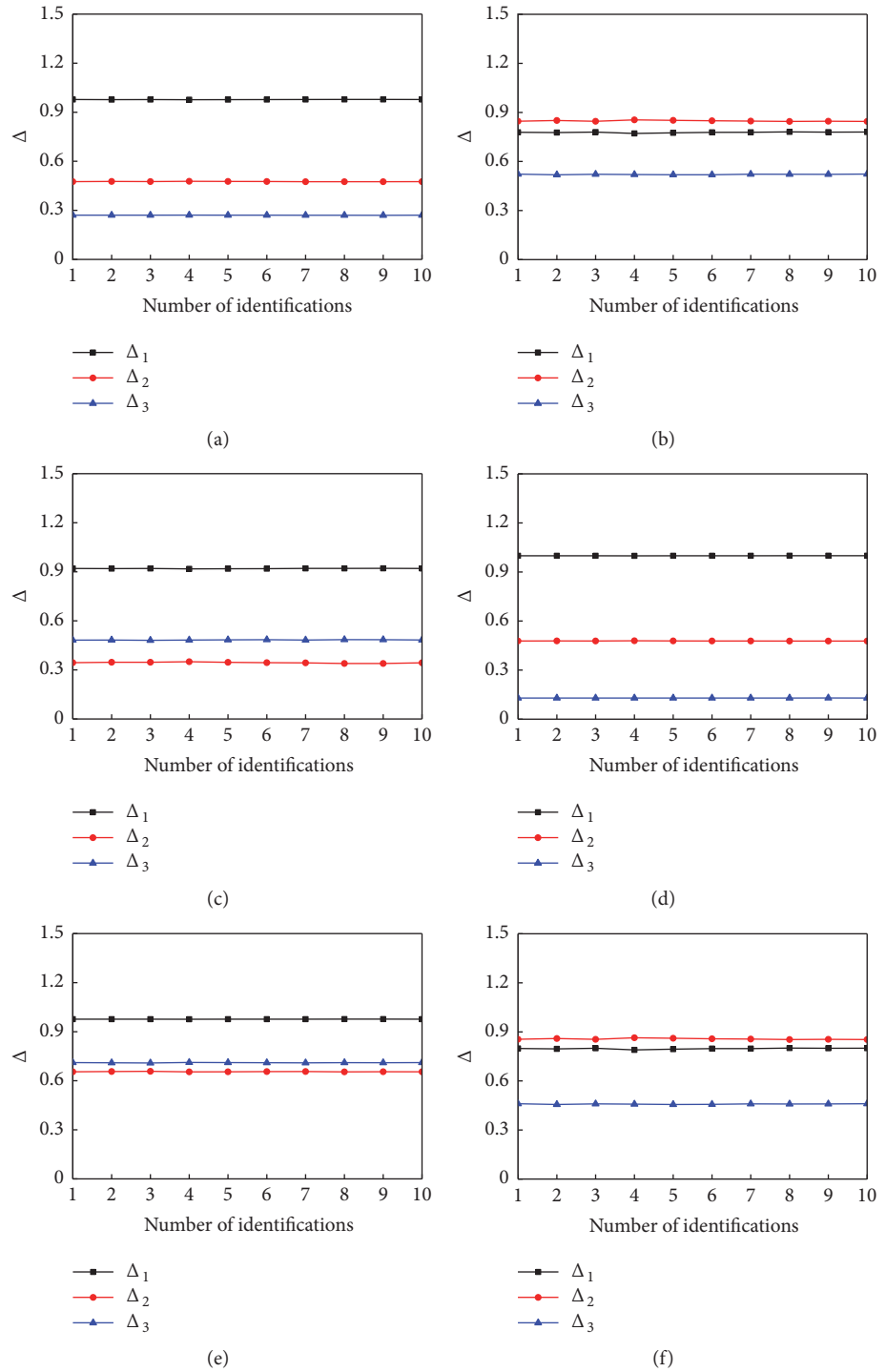

Figure 4: Δ value with different sensor placement. (a) Sensor set 1. (b) Sensor set 2. (c) Sensor set 3. (d) Sensor set 4. (e) Sensor set 5. (f) Sensor set 6.

Table 5: The mean values of Δ with 10% measurement noise.

$\overline{\Delta}$	Sensor set 1	Sensor set 2	Sensor set 3	Sensor set 4	Sensor set 5	Sensor set 6
$\overline{\Delta}_1$	0.9775	0.7779	0.9198	0.9991	0.9765	0.7975
$\overline{\Delta}_2$	0.4760	0.8480	0.3443	0.4781	0.6554	0.8568
$\overline{\Delta}_3$	0.2703	0.5210	0.4832	0.1293	0.7103	0.4585

Table 6: Identification results with proposed method.

Damping ratio	Sensor set 1		Sensor set 2		Sensor set 3	
	Mean value	Coefficient of variation	Mean value	Coefficient of variation	Mean value	Coefficient of variation
ζ_1	0.0100	0.0476	0.0099	0.2411	0.0102	0.0907
ζ_2	0.0200	0.0071	0.0200	0.0305	0.0200	0.0134
Damping ratio	Sensor set 4		Sensor set 5		Sensor set 6	
	Mean value	Coefficient of variation	Mean value	Coefficient of variation	Mean value	Coefficient of variation
ζ_1	0.0098	0.0921	0.0111	0.1869	0.0099	0.2765
ζ_2	0.0200	0.0114	0.0203	0.0287	0.0200	0.0349

Table 7: Identification results with conventional method.

Damping ratio	Sensor set 1		Sensor set 2		Sensor set 3	
	Mean value	Coefficient of variation	Mean value	Coefficient of variation	Mean value	Coefficient of variation
ζ_1	0.0127	0.2172	0.0090	0.2416	0.0124	0.1893
ζ_2	0.0208	0.0387	0.0197	0.0329	0.0207	0.0330
Damping ratio	Sensor set 4		Sensor set 5		Sensor set 6	
	Mean value	Coefficient of variation	Mean value	Coefficient of variation	Mean value	Coefficient of variation
ζ_1	0.0098	0.4422	0.0122	0.2041	0.0091	0.2913
ζ_2	0.0199	0.0567	0.0206	0.0328	0.0197	0.0378

information of damping ratio in every principal component is stable for all the sensor placements with measurement noise, and the damping perturbation information distribution is similar to that without measurement noise. The mean values $\overline{\Delta}_j$ for different sensor placements are shown in Table 5, and they are close to the ratio Δ_j of the "measured responses without noise effect".

Based on the above discussions the lower principal components contain more perturbation information of damping ratios and less measurement noise information, so the identification equation based on the lower order principal component will give more accurate identification result considering the measurement noise. The first-order principal component is adopted to identify the damping ratios, and ten different measurement noise series are considered for each sensor placement. The ten identification results are shown in Figure 5 with the proposed method and conventional sensitivity method, and it can be seen that the proposed method can give more accurate and stable identification result than the conventional method.

The mean values and coefficients of variation of the identification results with the proposed method are shown in Table 6, and those of the identification results with the conventional response sensitivity are shown in Table 7. Comparing the mean values in Table 6 with those in Table 7, the mean values of the identification results from proposed method are closer to the true value, so it can be concluded that the proposed method can give more accurate identification results.

Comparing the coefficients of variation in Table 6 with those in Table 7, the coefficients of variation, which can represent the standardized measure of dispersion, for identification results from the proposed method are much smaller than those in Table 7, so it shows that the proposed method can give more stable identification results.

3.4. Damping Identification with Different Measurement Noise Level. In this section 20% and 30% measurement noise levels are considered to investigate the performance of the proposed method under higher level measurement noise, and the identification results are compared with the conventional response sensitivity method. The evolution of damping ratios in these two noise level scenarios with different sensor placements is shown in Figure 6, and the finial identified results are shown in Table 8. The identification results in Figure 6 and Table 8 with 20% and 30% noise levels indicate that the

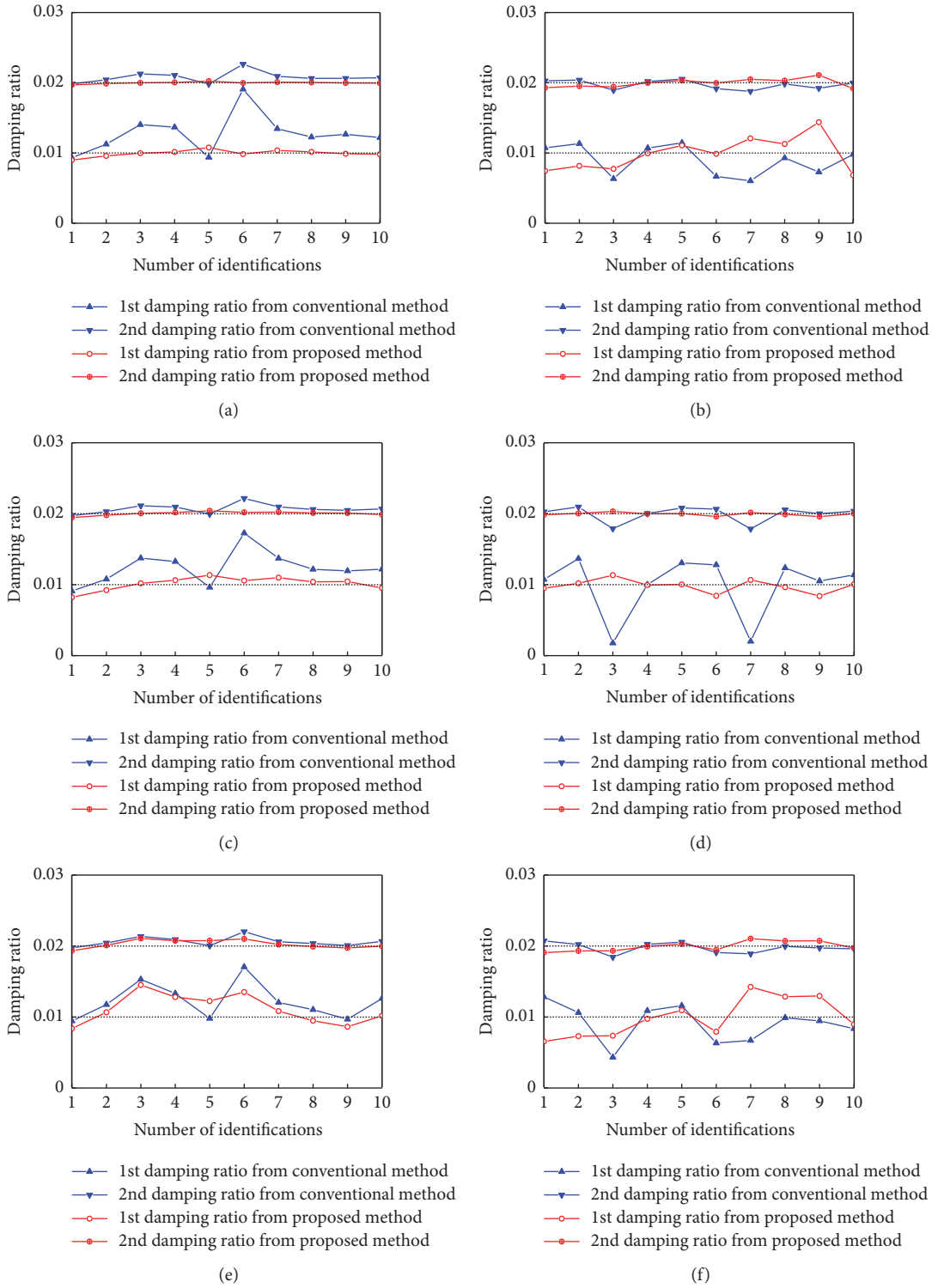

FIGURE 5: Identification results with different sensor placement with 10% measurement noise. (a) Sensor set 1. (b) Sensor set 2. (c) Sensor set 3. (d) Sensor set 4. (e) Sensor set 5. (f) Sensor set 6.

sensor placement effect is not significant for the proposed method, but for the conventional method the difference of the identification results between different sensor placements is much larger.

The damping ratio identification results show that the proposed method can identify the damping ratio with acceptable accuracy even under 30% measurement noise, and the difference of identification results between different noise

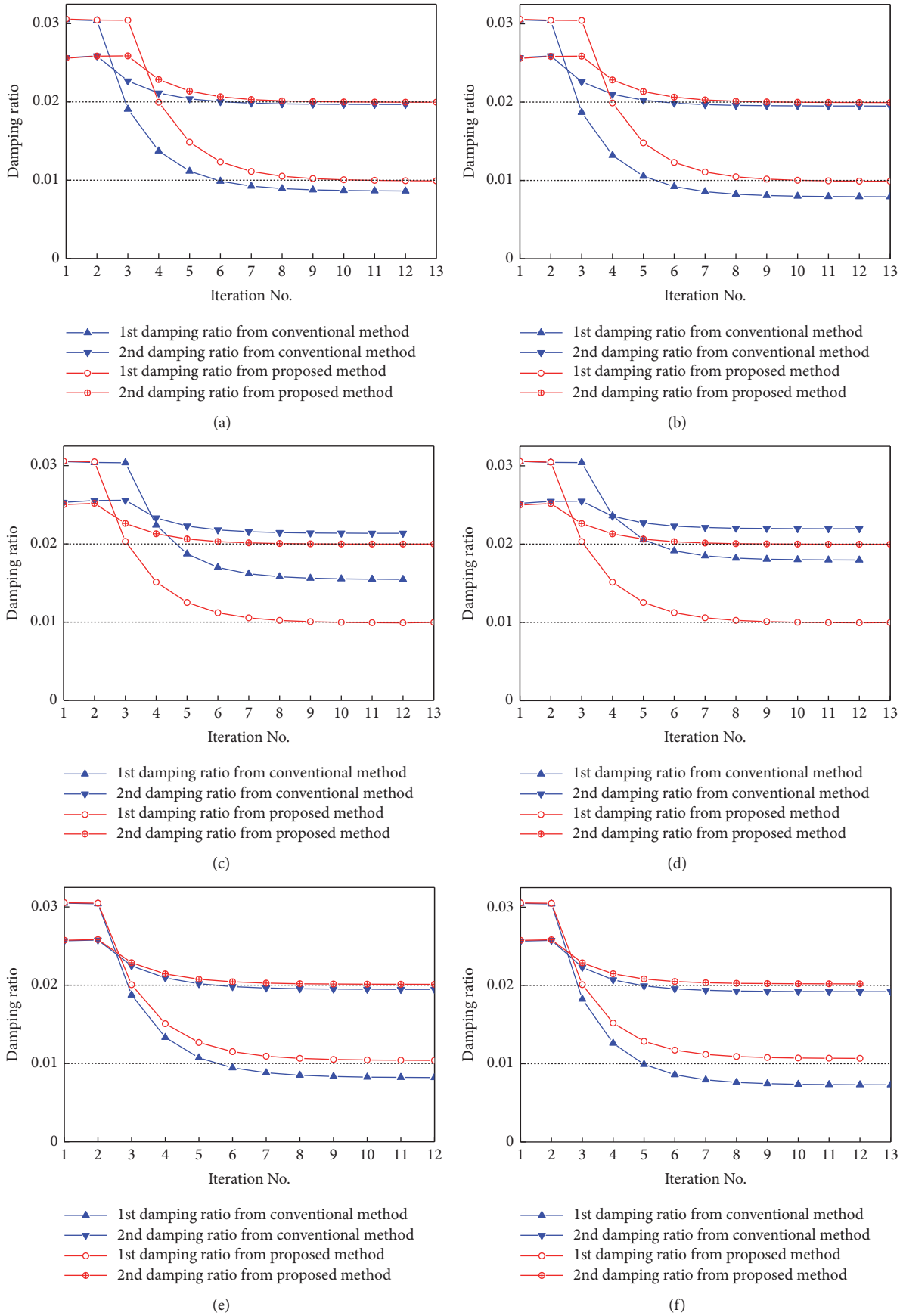

Figure 6: Continued.

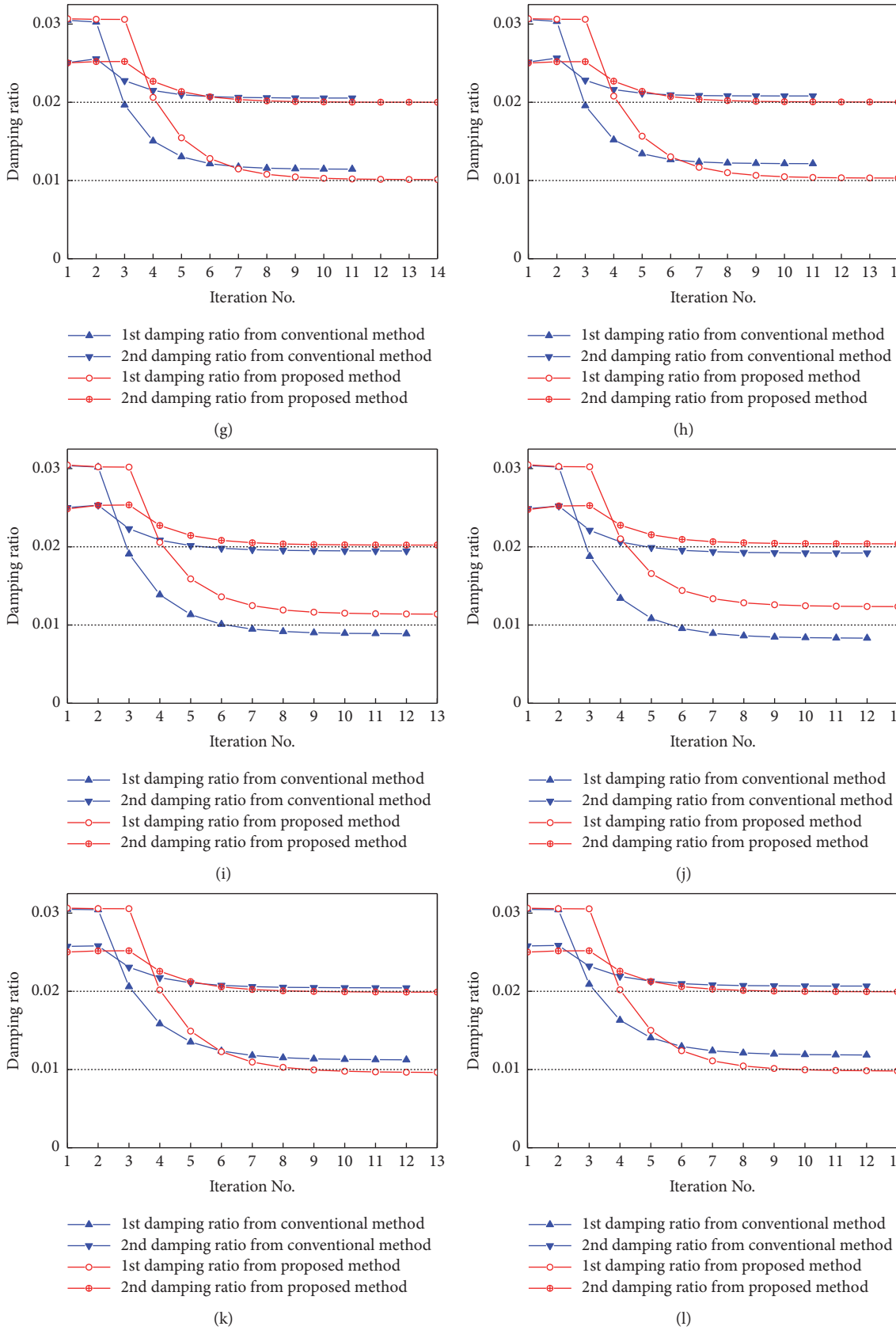

FIGURE 6: Evolution of identification from measured responses with different noise level. (a) Sensor set 1 with 20% noise. (b) Sensor set 1 with 30% noise. (c) Sensor set 2 with 20% noise. (d) Sensor set 2 with 30% noise. (e) Sensor set 3 with 20% noise. (f) Sensor set 3 with 30% noise. (g) Sensor set 4 with 20% noise. (h) Sensor set 4 with 30% noise. (i) Sensor set 5 with 20% noise. (j) Sensor set 5 with 30% noise. (k) Sensor set 6 with 20% noise. (l) Sensor set 6 with 30% noise.

Table 8: Identification results with 20% and 30% measurement noise.

Noise level	Damping ratio	Sensor set 1		Sensor set 2	
		Proposed method	Conventional method	Proposed method	Conventional method
20%	ζ_1	0.0099	0.0099	0.0099	0.0155
	ζ_2	0.0199	0.0199	0.0200	0.0214
30%	ζ_1	0.0099	0.0079	0.0099	0.0180
	ζ_2	0.0199	0.0195	0.0200	0.0220
Noise level	Damping ratio	Sensor set 3		Sensor set 4	
		Proposed method	Conventional method	Proposed method	Conventional method
20%	ζ_1	0.0104	0.0082	0.0101	0.0115
	ζ_2	0.0201	0.0195	0.0202	0.0205
30%	ζ_1	0.0107	0.0073	0.0103	0.0122
	ζ_2	0.0202	0.0192	0.0200	0.0208
Noise level	Damping ratio	Sensor set 5		Sensor set 6	
		Proposed method	Conventional method	Proposed method	Conventional method
20%	ζ_1	0.0114	0.0089	0.0096	0.0112
	ζ_2	0.0202	0.0195	0.0199	0.0204
30%	ζ_1	0.0124	0.0083	0.0098	0.0119
	ζ_2	0.2040	0.0192	0.0200	0.0207

Table 9: Weights of mass blocks.

Storey	Node number	Weight (kg)	Node number	Weight (kg)
1	5	3.986	8	3.907
2	13	3.967	16	3.946
3	21	3.934	24	3.944
4	29	3.966	32	3.937
5	37	3.940	40	3.952
6	45	3.944	48	3.923
7	53	3.940	56	3.958

levels is very small, which means the proposed method is less affected by measurement noise. With the increasing of the measurement noise level, the results from the conventional method become worse, and with 30% measurement noise the identification error of the conventional method is too large to be accepted.

4. Experimental Study

4.1. Experimental Model and Finite Element Modeling. A 7-storey planar steel frame is adopted to verify the proposed damping identification method in the laboratory, and more details of the test can be found in the thesis of the second author [26]. The configuration of the test model is shown in Figure 7. The measured mass densities of the column and beam materials are 7850kg/m3 and 7764kg/m3, respectively, and the measured cross sections of the column and beam elements are 50.06 mm × 5.10 mm and 49.88 mm × 8.06 mm, respectively. Additional mass blocks have been placed on the 1/4 and 3/4 length along the beam members to simulate the inertia of floor slab in practice, and the weights of mass blocks are listed in Table 9.

B&K 3023 accelerometers shown in Figure 8(a) and B&K Nexus amplifiers shown in Figure 8(b) were adopted to collect the acceleration responses. Impact test was performed with SINOCERA LC-04A dynamic hammer shown in Figure 8(c) to apply the impact excitation, and the National Instrument data acquisition board shown in Figure 8(d) was adopted to record data for the test.

To reduce the discrepancy between the analytical model and the experimental model, the initial finite element model is updated before the damping ratios identification. The baseline finite element model of the test structure is obtained from model updating with the modal sensitivity approach. Young's modulus for each element and the stiffness values for two restraints at the supports are updated, because the dimensions and mass can be measured in situ. The detailed procedure for the baseline model updating can be found in [26], in which the accuracy of the baseline finite element model is verified by the minimized errors in the Modal Assurance Criteria (MAC) values before and after updating.

4.2. Damping Identification of the Experimental Model. Based on the Rayleigh damping model assumption, the proposed method is adopted to identify the first two damping ratios of the test model. The measured acceleration responses of the test model under hammer impact force are adopted, and the hammer impact location and measurement locations are shown in Table 10. Both of the initial damping ratios for the first and second modes are set as 0.5%, and the analytical responses calculated by the assumed damping ratios and baseline finite element model are compared with the measured responses shown in Figures 9(a), 9(c), and 9(e).

Because the true values of the damping ratios of the test model are unknown, the relative errors between the measured responses and analytical responses with the identified

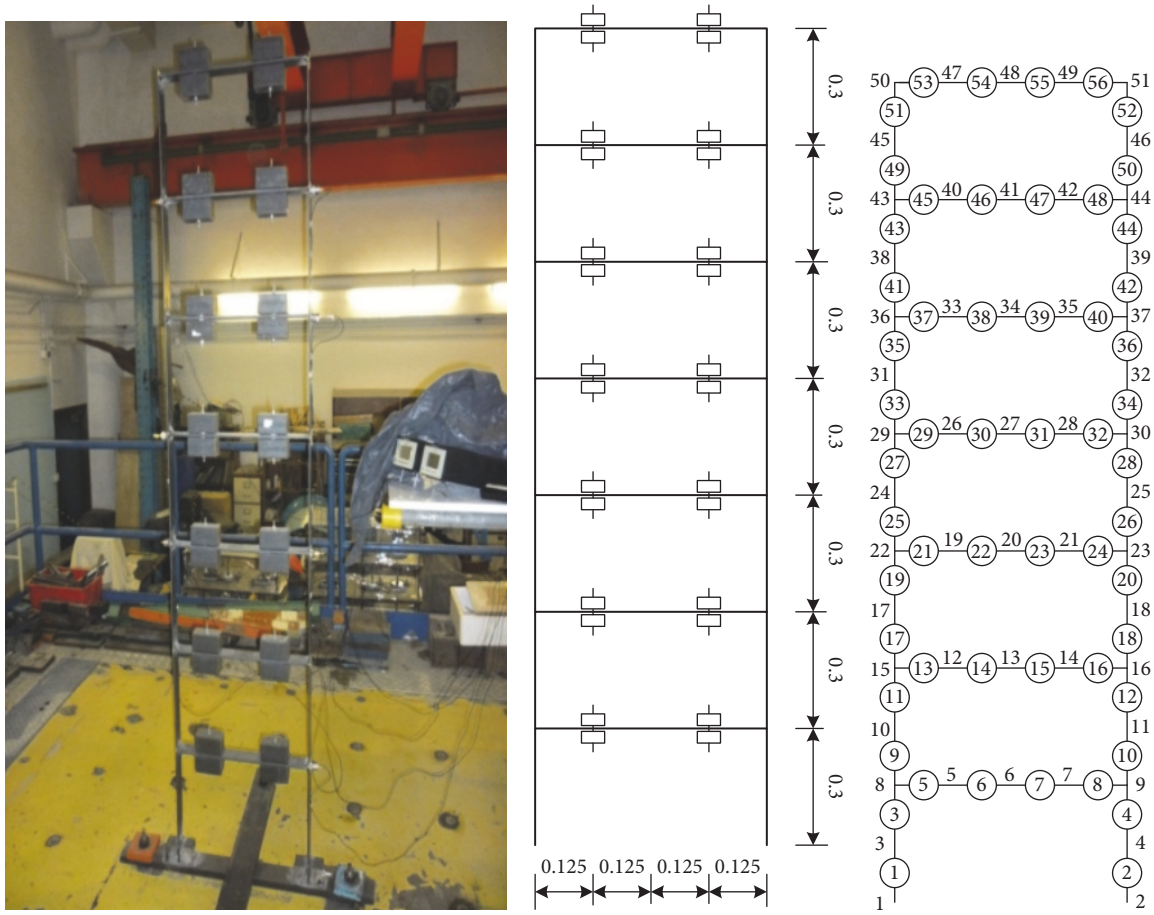

(a) (b) (c)

FIGURE 7: Test model and finite element model. (a) The test model in laboratory. (b) The dimensions of the test model. (c) The element and node numbering system of the finite element model.

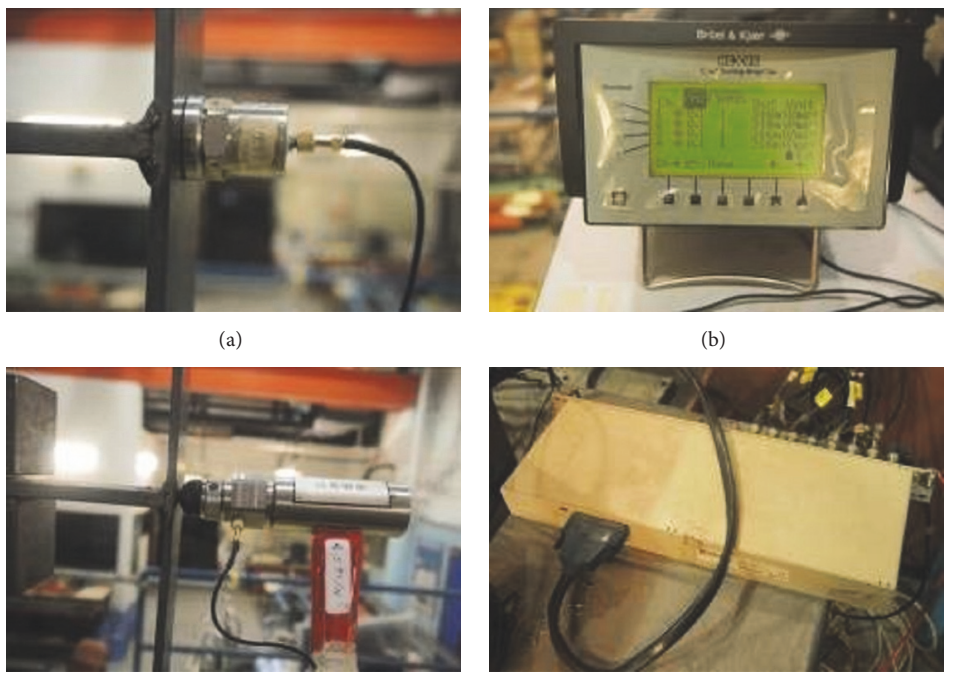

(a) (b)

(c) (d)

FIGURE 8: Instruments adopted in the test. (a) B&K 3023 accelerometer. (b) B&K Nexus amplifier. (c) Hammer. (d) NI data acquisition board.

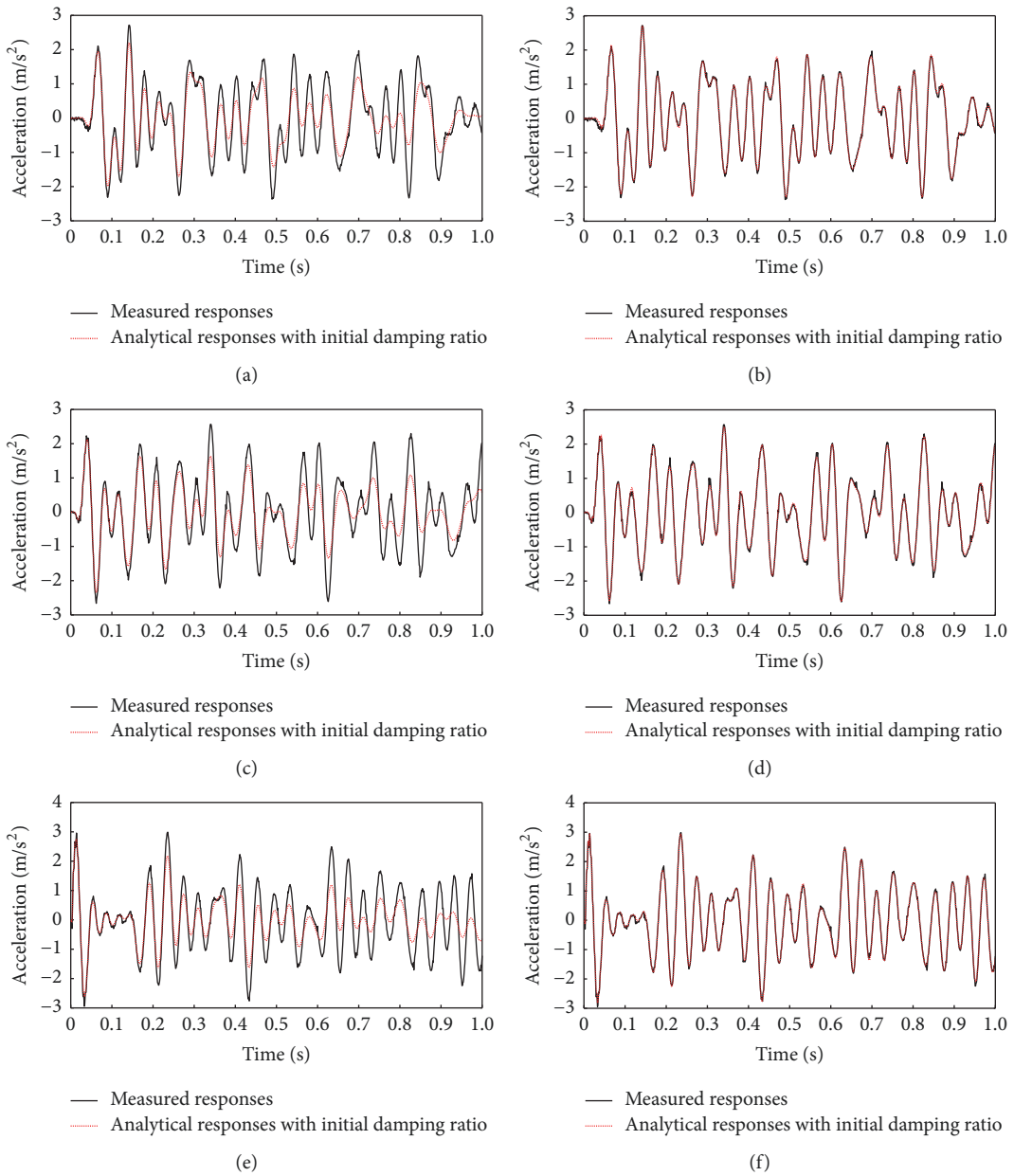

Figure 9: Comparison between the measured responses and the analytical responses. (a) Measured responses and analytical responses with the initial damping ratios at 43x. (b) Measured responses and analytical responses with the identified damping ratios at 43x. (c) Measured responses and analytical responses with the initial damping ratios at 29x. (d) Measured responses and analytical responses with the identified damping ratios at 29x. (e) Measured responses and analytical responses with the initial damping ratios at 15x. (f) Measured responses and analytical responses with the initial damping ratios at 15x.

Table 10: Location of impact load and accelerometer.

Type of Sensor	Location (Node)	Location (DOF)
Impact Load	50x	148
Accelerometer	43x	127
	29x	85
	15x	43

damping ratios are selected to represent the identification error. The damping ratios are identified as $\zeta_1 = 0.00173$ and $\zeta_2 = 0.00097$ with the proposed method, and the analytical responses calculated by the identified damping ratios and baseline finite element model are compared with the measured responses in Figures 9(b), 9(d), and 9(f).

The relative errors between the initial analytical responses and measured responses are shown in Table 11, and the corresponding relative errors between the analytical responses with the identified damping ratios and measured responses are also shown in Table 11. It shows that with the identified damping ratios the analytical responses match the measured responses very well and using the identified damping ratios

Table 11: The relative errors in the measured and analytical responses.

Sensor location (Node)	Error with assumed damping ratios	Error with identified damping ratios
43x	42.16%	4.94%
29x	43.32%	5.76%
15x	51.06%	5.53%

from the proposed approach to calculate the analytical response can give a smaller relative error in the dynamic response prediction compared with the experimental measured response.

5. Conclusions and Discussions

A damping identification method is proposed based on the combination of response sensitivity analysis and PCA method, in which the response sensitivity equation is projected into the subspace constructed by the first principal component of the measured responses. The first principal component of the measured responses contains more damping ratio variation information and less noise information, so the measurement noise effect is reduced significantly and the sensitivity of the measured response is enhanced simultaneously by the projection. This proposed method is validated in numerical studies with a planar truss structure with up to 30% measurement noise, and the enhanced sensitivity method performs better compared to the conventional sensitivity-based method for damping ratio identification. With a steel place frame, the proposed method is also validated experimentally, and the identification results also provide experimental evidences to support conclusions drawn above.

It should be noted that the Rayleigh damping model is adopted in this paper, and the damping ratios in Rayleigh damping model are identified based on the proposed method. A generalized projection method was proposed, so we can use similar procedure to identify the damping parameters in other types of damping model. It should also be noted that the identification results of the proposed method have some variations with different sensor placements under high level measurement noise, so the sensor placement effect and improved damping identification method should be studied later.

Data Availability

The data used to support the findings of this study are available from the corresponding author upon request.

Disclosure

The funding sponsors had no role in the design of the study; in the collection, analyses, or interpretation of data; in the writing of the manuscript; and in the decision to publish the results.

Conflicts of Interest

The authors declare no conflicts of interest.

Acknowledgments

The work described in this paper was supported by "Financial Grant from the China Postdoctoral Science Foundation" (Grant no. 2015M580267; Grant no. 2016T90296) and "National Natural Science Foundation of China" (Grant no. 51708159; Grant no. 51008094). The Ph.D. thesis of the second author [26] provided theoretical foundation for this paper.

References

[1] A. K. Chopra, *Dynamics of structures: Theory and Applications to Earthquake Engineering*, Prentice Hall, New Jersey, NY, USA, 2012.

[2] D. F. Pilkey, *Computation of a damping matrix for finite element model updating [Ph.D. thesis]*, Virginia Polytechnic Institute and State University, Blacksburg, Virginia, Va, USA, 1998.

[3] W. Wang, Q. Li, J. Gao, J. Yao, and P. Allaire, "An identification method for damping ratio in rotor systems," *Mechanical Systems and Signal Processing*, vol. 68, pp. 536–554, 2015.

[4] D. E. Holland and B. I. Epureanu, "A component damping identification method for mistuned blisks," *Mechanical Systems and Signal Processing*, vol. 41, no. 1-2, pp. 598–612, 2013.

[5] C. Devriendt, P. J. Jordaens, G. De Sitter, and P. Guillaume, "Damping estimation of an offshore wind turbine on a monopile foundation," *IET Renewable Power Generation*, vol. 7, no. 4, pp. 401–412, 2013.

[6] B. A. Olmos and J. M. Roesset, "Evaluation of the half-power bandwidth method to estimate damping in systems without real modes," *Earthquake Engineering & Structural Dynamics*, vol. 39, no. 14, pp. 1671–1686, 2010.

[7] G. A. Papagiannopoulos and G. D. Hatzigeorgiou, "On the use of the half-power bandwidth method to estimate damping in building structures," *Soil Dynamics and Earthquake Engineering*, vol. 31, no. 7, pp. 1075–1079, 2011.

[8] I. Wang, "An analysis of higher order effects in the half power method for calculating damping," *Journal of Applied Mechanics*, vol. 78, no. 1, p. 014501, 2011.

[9] X. Y. Li and S. S. Law, "Identification of structural damping in time domain," *Journal of Sound and Vibration*, vol. 328, no. 1-2, pp. 71–84, 2009.

[10] Y. Ding and S. S. Law, "Structural damping identification based on an iterative regularization method," *Journal of Sound and Vibration*, vol. 330, no. 10, pp. 2281–2298, 2011.

[11] T. Uhl and A. Klepka, "Application of wavelet transform for identification of modal parameters of nonstationary systems," *Journal of Linguistic Anthropology*, vol. 12, no. 1, pp. 99–101, 2005.

[12] J. Li, H. Hao, and G. Fan, "Numerical and experimental verifications on damping identification with model updating and vibration monitoring data," *Smart Structures and Systems*, vol. 20, no. 2, pp. 127–137, 2017.

[13] H. Zhang, J. Yang, and L. Xiao, "Damping ratio identification using a continuous wavelet transform to vortex-induced motion of a Truss Spar," *Ships and Offshore Structures*, vol. 9, no. 6, pp. 596–604, 2014.

[14] Y. L. Xu, S. W. Chen, and R. C. Zhang, "Modal identification of Di Wang building under Typhoon York using the Hilbert-Huang transform method," *Structural Design of Tall Buildings*, vol. 12, no. 1, pp. 21–47, 2003.

[15] A. Saltelli, K. Chan, and E. M. Scott, *Sensitivity Analysis*, John Wiley and Sons Inc, New York, NY, USA, 2000.

[16] A. Saltelli, S. Tarantola, and F. Campolongo, *Sensitivity analysis in practice: a guide to assessing scientific models*, John Wiley and Sons Inc, Hoboken, New Jersey, USA, 2004.

[17] T. Turanyi, "Sensitivity analysis of complex kinetic systems. Tools and applications," *Journal of Mathematical Chemistry*, vol. 5, no. 3, pp. 203–248, 1990.

[18] A. Saltelli, S. Tarantola, and F. Campolongo, "Sensitivity analysis as an ingredient of modeling," *Statistical Science*, vol. 15, no. 4, pp. 377–395, 2000.

[19] R. Serban and L. R. Petzold, "Efficient computation of sensitivities for ordinary differential equation boundary value problems," *SIAM Journal on Numerical Analysis*, vol. 40, no. 1, pp. 220–232, 2002.

[20] Z. R. Lu and S. S. Law, "Features of dynamic response sensitivity and its application in damage detection," *Journal of Sound and Vibration*, vol. 303, no. 1-2, pp. 305–329, 2007.

[21] Z. R. Lu and S. S. Law, "Identification of system parameters and input force from output only," *Mechanical Systems and Signal Processing*, vol. 21, no. 5, pp. 2099–2111, 2007.

[22] C.-H. Loh, C.-H. Mao, J.-R. Huang, and T.-C. Pan, "System identification and damage evaluation of degrading hysteresis of reinforced concrete frames," *Earthquake Engineering & Structural Dynamics*, vol. 40, no. 6, pp. 623–640, 2011.

[23] K. Liu, S.-S. Law, and X.-Q. Zhu, "Sensitivity enhancement for structural condition assessment with noisy excitation or with only output," *International Journal of Structural Stability and Dynamics*, vol. 15, no. 6, article 1450083, 2015.

[24] K. Liu, S. S. Law, Y. Xia, and X. Q. Zhu, "Singular spectrum analysis for enhancing the sensitivity in structural damage detection," *Journal of Sound and Vibration*, vol. 333, no. 2, pp. 392–417, 2014.

[25] K. Liu, S. S. Law, and X. Q. Zhu, "System parameter identification from projection of inverse analysis," *Journal of Sound and Vibration*, vol. 396, pp. 83–107, 2017.

[26] K. Liu, *Structural condition assessment with incomplete noisy acceleration measurements*, The Hong Kong Polytechnic University, 2014.

[27] W. J. Krzanowski, *Principles of Multivariate Analysis-A User'S Perspective*, Oxford University Press, New York, NY, USA, 2000.

[28] L. A. Prendergast, "A note on sensitivity of principal component subspaces and the efficient detection of influential observations in high dimensions," *Electronic Journal of Statistics*, vol. 2, pp. 454–467, 2008.

[29] M. A. Perry, H. P. Wynn, and R. A. Bates, "Principal components analysis in sensitivity studies of dynamic systems," *Probabilistic Engineering Mechanics*, vol. 21, no. 4, pp. 454–460, 2006.

[30] P. C. Hansen, "Analysis of discrete ill-posed problems by means of the *L*-curve," *SIAM Review*, vol. 34, no. 4, pp. 561–580, 1992.